EFFECT OF INHIBITOR-LOADED HALLOYSITE NANOTUBES AND MONTMORILLONITE CLAY NANOCONTAINERS FOR SELF-HEALING CORROSION PROTECTION OF ALUMINUM ALLOY 2024-T4

Manasa SAMAVEDAM [1,2] Vengatajalabathy Gobi KAUVERI [2], Subasri RAGHAVAN[1*]

[1] *International Advanced Research Centre for Powder Metallurgy and New Materials (ARCI), Centre for Sol-Gel Coatings, Balapur, Hyderabad - 500005, Telangana State, India*
[2] *National Institute of Technology Warangal, Department of Chemistry, Warangal-506004, Telangana State, India*
[*] *Corresponding author: Subasri Raghavan (subasri@arci.res.in)*

Abstract: *A combination of halloysite (H) and montmorillonite (M) nanoclays loaded with Ce^{3+} and Zr^{4+} cationic corrosion inhibitors as the self-healing smart nanocontainers for the corrosion protection of AA2024-T4 alloy was investigated. Two different coating systems i) Bilayer (H|M and M|H) and composite coatings (M+H), were developed using these two inhibitor-loaded nanocontainers. The loaded nanocontainers were dispersed in a hybrid silane matrix. Coatings were applied on AA2024-T4 substrates by the dip coating technique, followed by curing at 130 °C. The corrosion protection performance of these coatings was studied by electrochemical tests and salt spray analyses. Self-healing behavior of coatings was investigated using a salt immersion test by making an artificial scratch on the substrate. Bilayer M|H coatings have provided enhanced and prolonged corrosion protection than composite coatings due to the controlled release of cationic corrosion inhibitors from inner M and outer H nanocontainers.*

Keywords: *Halloysite nanotubes, montmorillonite nanoclay, cationic corrosion inhibitors, sol-gel matrix, self-healing coatings, corrosion protection.*

1. Introduction

AA2024-T4 aluminum alloy is widely used in aircraft applications in making various structural parts of the aircraft body, due to its light weight and high strength properties. These alloys are generally protected by a thin layer of Al_2O_3. However, this Cu rich alloy is prone to corrosion during its usage, consequently leading to a huge metal loss [1]. Therefore, these surfaces need corrosion protection. Cr (VI) conversion coatings, though, are the most effective coatings, but are carcinogenic in nature, therefore banned worldwide [2]. Hence, there is an increased demand for developing alternative chrome-free and eco-friendly coatings. Sol-gel coatings are known to be the most effective replacements, as they possess various properties like good barrier protection, excellent adhesion strength, hardness, and flexibility. In addition, they can be easily deposited and require very low temperatures for their densification [3]. Incorporation of corrosion inhibitors into the sol-gel matrix enhances the anticorrosive property, but it was found from the literature that direct addition of an inhibitor into the sol-gel matrix leads to deterioration of the coating [4]. Hence, encapsulation of inhibitors into nanocontainers is a new approach for developing self-healing coatings. This avoids the uncontrolled leakage of corrosion inhibitors and releases the inhibitors only on the onset of damage to the coating. Therefore, they are termed as smart coatings. Clay nanotubes [5], polymeric microcapsules [6], carbon nanotubes [7], layered double hydroxides[8], and montmorillonite clay [9] have been widely investigated as nanocontainers.

However, research on the use of a combination of two or more smart nanocontainers is emerging and is a recent strategy for the development of corrosion protection coatings for prolonged durations. Darmiani *et al.* [10] have studied the synergistic effect of montmorillonite and cerium nitrate nanocomposite-based epoxy coatings on cold-rolled steel panels. Montemor *et al.* [11] have used the combination of layered double hydroxides (LDH) and cerium molybdate hollow spheres loaded with mercaptobenzothiazole. They reported that the combination of two nanocontainers resulted in synergistic corrosion inhibition. Serdechnova *et al.* [12] have used a combination of LDH and bentonite with two different inhibitors 1,2,3-benzotriazole and Ce^{3+}. These coatings were found

to show good corrosion protection and self-healing ability due to the synergistic effect of different inhibitors loaded nanocontainers for galvanically coupled aluminum alloy AA6061 with carbon fiber reinforced plastic. From the above-reported literature, it was observed that the use of two or more inhibitors and/or nanocontainers was found to be immensely effective in protecting metal surfaces due to their synergistic behavior.

To the best of our knowledge, there is no reported literature on the use of a combination of corrosion inhibitor-loaded nanocontainers with tubular structure like halloysite nanotubes (HNT) and layered structure like montmorillonite nanoclays (MMT). In this context, the present investigation was carried out to study the effect of a combination of cationic inhibitors Ce^{3+} and Zr^{4+} loaded HNT and MMT nanocontainers dispersed in an organic-inorganic hybrid silane matrix on the corrosion protection behavior of AA2024-T4 alloy.

2. Experimental

2.1 Preparation of sols and deposition of coatings

Materials required for the preparation of inorganic-organic hybrid matrix sol, nanocontainers, and corrosion inhibitors, and the synthesis procedure for matrix sol, loading of cationic corrosion inhibitors Ce^{3+} and Zr^{4+} into HNT and MMT clays was carried out as mentioned in our previous reports [9,13,14].

The Ce^{3+} and Zr^{4+} inhibitors loaded MMT and HNT were used to make two different types of coatings: i) The inhibitors loaded HNT and MMT powders were mixed in 1:1 wt ratio and then dispersed in a hybrid sol-gel matrix to synthesize a composite sol, which is labeled as M+H. ii) Inhibitors loaded HNT and MMT powders dispersed individually in matrix sol and applied as bilayer coatings, in two different configurations, such as i) M|H Coating and ii) H|M coating. Moreover, HNT and MMT nanocontainers without inhibitors (unloaded nanocontainers) have also been dispersed in matrix sol in the same wt % as that of inhibitor-loaded nanocontainers and are abbreviated as HNC sol and MNC sol, respectively. All the coatings were applied on AA2024-T4 substrates by the dip coating technique at 1 [mm s^{-1}] withdrawal speed. Coated substrates were cured at 130 $^{\circ}$C for 1 h, and in the case of bilayer coatings, the first layer was cured before applying the next layer of coating.

2.2 Characterization and testing

A transmission electron microscope (TEM, Tecnai 200 G2, FEI, Netherlands) was used to confirm the loading of corrosion inhibitors into HNT and MMT. EIS and Potentiodynamic polarization experiments performed using a CH instrument, USA (Model 604E) for coated and uncoated substrates, with detailed characterization details as mentioned in ref. [9]. Salt spray test was performed by exposing the uncoated and coated substrates to 5 wt % NaCl solution for 168 h according to ASTM B117-16 standard [15]. Salt immersion test was performed by making an artificial ‘X’ shaped damage on the substrates and immersing them in 3.5 wt % NaCl solution for 5 days [16, 17]. EDS elemental mapping was carried out before and after immersion time to observe the release of corrosion inhibitors into the damaged area.

3. Results and Discussion

3.1 Morphology, composition of nanocontainers, and Thickness of coatings

Ce and Zr-loaded HNT and MMT clays appeared as tubular and layered structures when seen through TEM, as given in Figures 1 (a) and (b), respectively. EDS analysis of the loaded

nanocontainers, as presented in Table 1, showed the presence of Ce and Zr along with Al, Si, and O in both the nanocontainers. This confirmed the loading of corrosion inhibitors in both nanocontainers.

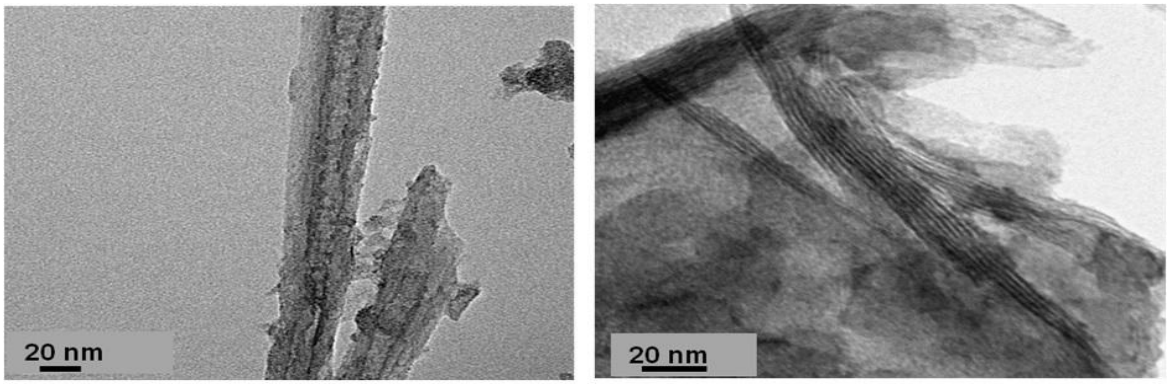

Figure 1. TEM images of inhibitor-loaded (a) HNT and (b) MMT nanocontainers.

Table 1. Weight ratio (%) of different elements obtained from EDS analysis.

Name of the sample	O	Na	Mg	Cu	Al	Si	Zr	Ce
Inhibitors loaded Halloysite	65.18	1.08	-	2.12	10.91	18.27	2.28	0.16
Inhibitors loaded Montmorillonite	43.41	-	5.76	1.64	19.58	25.50	3.63	0.48

All the coatings were seen to be adherent to the substrates, and their thickness is given in Table 2. It can be observed from Table 2 that M|H coating has shown nearly an equal thickness for both inner and outer layers and was less thick than H|M coating. This observation clearly infers that the presence of montmorillonite for coatings intended to form always thinner inner coatings on the AA2024-T4 alloy substrate.

Table 2. Thickness of bilayer and composite coatings

Name of the coating	M|H		H|M		M+H
Thickness (µm)	Inner M layer	Outer H layer	Inner H layer	Outer M layer	3.8 (±0.1)
	2.9 (±0.3)	3.8 (±0.1)	4.6 (±0.3)	8.4 (±0.2)	
	Total Thickness = 6.8 (±0.2)		Total thickness = 13.2 (±0.4)		

3.2 Electrochemical impedance spectroscopy (EIS) and potentiodynamic polarization studies

EIS and potentiodynamic polarization studies were carried out for bare AA2024-T4, H|M, and M|H and M+H coated substrates after 1, 72, 120 h, and were further extended to 168 and 216 h of exposure to 3.5 wt % NaCl solution for M|H and M+H coated substrates. The EIS and polarization results of these coatings were compared with those of single-layer H and M-coated substrates.

The equivalent electrical circuit used for fitting the EIS data of bilayer coatings is given in Figure 2 (a), and for composite and single-layer coatings is given in Figure 2 (b).

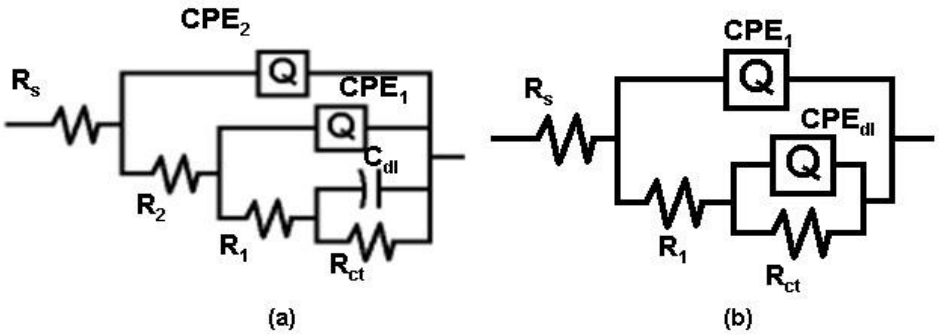

Figure 2. Equivalent electric circuits used for fitting EIS data of (a) bilayer coatings and (b) composite and single-layer M and H coatings

A comparison of charge transfer resistance (R_{ct}) obtained from EIS data of all coated and bare AA2024-T4 substrates is shown in Figure 3 (a). M|H coated substrates exhibited the highest R_{ct} among all coatings, at all durations of exposure. In contrast, H|M coated substrates exhibited lower R_{ct} values than those of M|H and M+H coated substrates. From the above observations, the M|H configuration was found to have better corrosion protection than H|M coatings. Therefore, the EIS studies were carried out further for only M|H coatings till 216 h. On the other hand, the M+H coatings exhibited better R_{ct} than H|M coatings but exhibited lower R_{ct} than single-layer H and M coatings. These observations clearly indicate that there was no improvement in the corrosion protection after making the composite coating compared to single-component H and M coatings. It can also be observed from Figure 3 (a) that the R_{ct} values of M|H coatings drastically decreased till 120 h and increased after prolonged exposure to 168 h, and remained almost the same after 216 h. This indicates that there could have been an initiation of corrosion due to the penetration of Cl^- ions (from 3.5 wt % NaCl solution), which in turn triggered the self-healing action to increase the R_{ct} at the interface after prolonged duration.

The single-layer H exhibited higher R_{ct} than all except M|H, but it decreased after the prolonged duration of exposure for 216 h (as observed in Figure 3 (a)). Single-layer M showed better coating resistance (R_1) than that of H. This clearly indicates that M|H coated substrates exhibited enhanced corrosion protection because of the inner M having better coating resistance and the outer H layer exhibiting good R_{ct}.

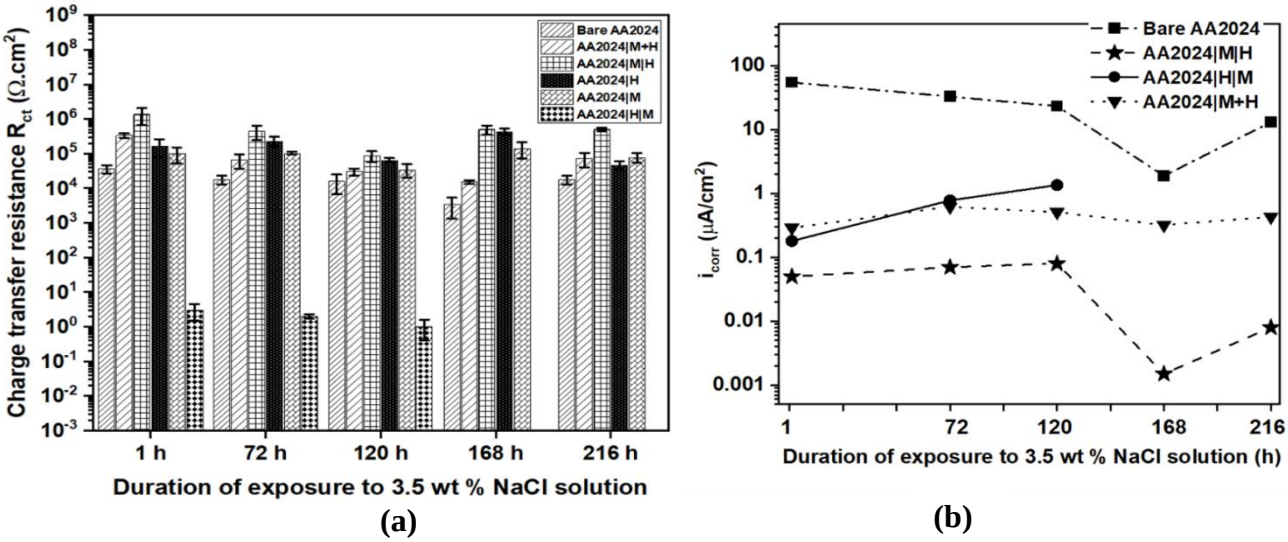

Figure 3. Comparison of (a) R_{ct} from EIS data and (b) i_{corr} from polarization data at different durations of exposure to corrosive medium.

The I_{corr} data obtained from potentiodynamic polarization plots after different exposure durations, shown in Figure 3 (b), follow a similar trend as that of EIS data. The least corrosion currents (i_{corr}) were measured for M|H coating at all durations of exposure. In addition, it has also been observed that the M|H coating exhibited more positive corrosion potential values (E_{corr}) compared to all the coated substrates. This indicates that there is an ennoblement of corrosion potentials.

The enhanced corrosion protection of M|H over H|M coating, though both are of bilayer configuration, motivated us to study the reason for this behavior. Hence, in this context, the corrosion protection behaviour of the coatings developed from unloaded HNT and MMT nanocontainers, i.e., HNC and MNC, was investigated. The HNC-coated substrates exhibited lower i_{corr} than MNC initially (1 h), but as the exposure duration increased to 72 and 120 h, MNC coatings exhibited lower i_{corr} values than HNC, as shown in Figure 4 (a). The coating resistance (R_1) values of MNC-coated substrates were found to be higher than HNC (data not presented here). This indicates that MMT nanocontainers, when present as an adjacent layer to the substrate, provided good corrosion protection when compared to HNT as the adjacent coating to the substrate.

The variation in the behavior of coatings based on the two unloaded nanocontainers was found to be attributed to the orientation of these nanoparticles in the matrix sol as reported by Huttunen-Saarivirta et al [18]. They have dispersed HNT and MMT independently in an epoxy matrix and studied the corrosion protection of coatings on cold-rolled steel substrates and on aluminum foil. According to their findings, HNT nanoparticles get oriented randomly in the epoxy matrix, resulting in increased water permeability. However, MMT clay, when dispersed in the epoxy matrix, oriented itself parallel to the coating surface, thus exhibiting less water permeability and providing good coating and corrosion resistance. The schematic representation of HNC and MNC coatings and comparison of their coating resistance is depicted in Figure 4 (b).

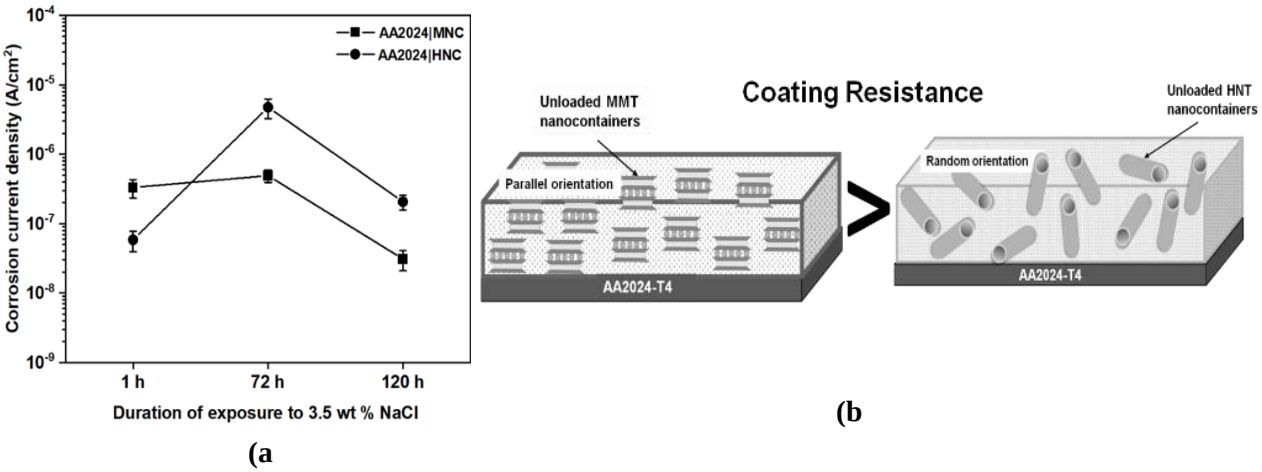

Figure 4. (a) Variation of i_{corr} of HNC and MNC coated AA2024-T4 substrates at different exposure durations, (b) schematic representation of comparison of coating resistance of MMT and HNT nanocontainers based coatings.

Therefore, based on the above observations, the improved corrosion protection of M|H coatings over H|M, can be explained because of the inner M layer containing MMT nanocontainers, which had a good coating resistance, and the outer H layer with HNTs having higher R_{ct}. These two nanocontainers as M|H configuration, exhibited enhanced release of the corrosion inhibitors and provided prolonged corrosion protection to the substrate, due to the combined effect of both the nanocontainers, which release inhibitors from each layer only on demand (on the onset of damage to the coating). The above conclusions were supported by results obtained for salt spray test (SST) as well as the salt immersion test (SIT), as shown in Figures 5 and 6. The results from electrochemical as well as salt spray tests confirmed that the cationic corrosion inhibitors have been released from the nanocontainers into the scratch region to self-heal the damage by forming passive layers of CeO_2 and ZrO_2.

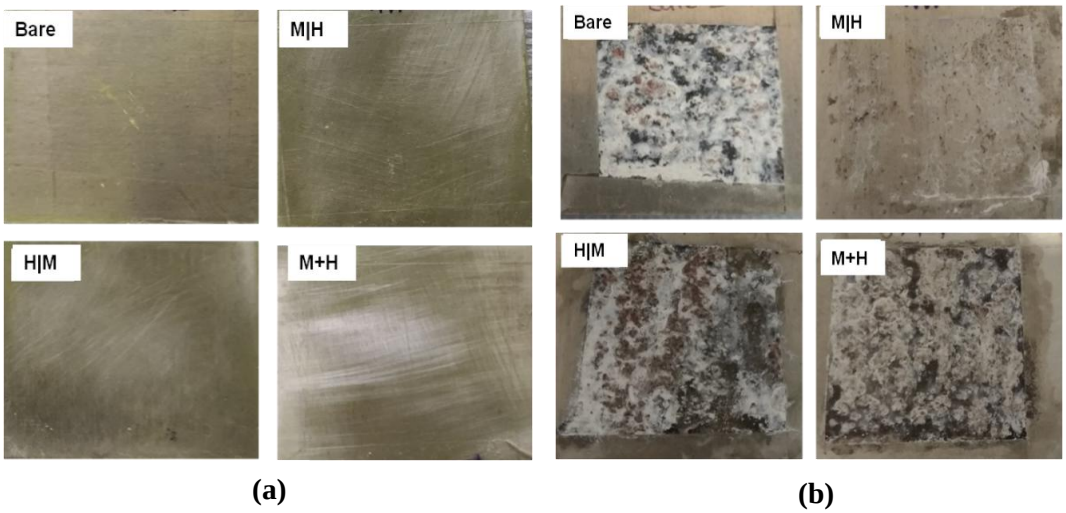

Figure 5. Photographs of AA2024-T4 substrates (a) before and (b) after SST for 168 h.

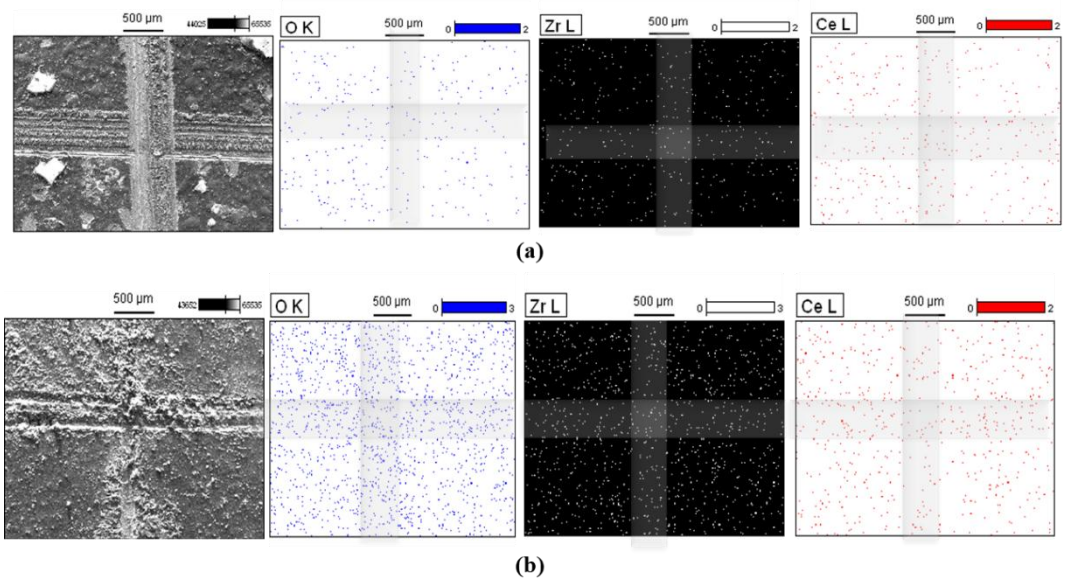

Figure 6. Elemental mapping of M|H coated substrates (a) before and (b) after SIT.

4. Conclusions

The improved corrosion resistance of M|H coatings on AA2024-T4 was explained based on the combined effect of both MMT and HNT nanocontainers, resulting in enhanced and controlled release of the corrosion inhibitors to heal the damage by formation of ceria and zirconia passive layers. Selectively designed bilayer coatings were found advantageous for prolonged and enhanced corrosion protection, and thus novel bilayer coatings with different combinations, organic/inorganic inhibitors, different nanocontainers, etc., need to be explored further to achieve highly promising and efficient self-healing coatings.

5. Acknowledgements

The authors would like to acknowledge the constant support provided by Director, ARCI, Hyderabad, throughout the course of this investigation. The authors thank M. Ramakrishna for carrying out TEM analysis.

References

[1] Svenningsen, G., Corrosion of Aluminium Alloys, *Department of Material Technology, 1 (1992),* pp. 7491.

[2] Zhao, J., Xia, L., Sehgal, A., Lu, D., Frankel GS, Effects of chromate and chromate conversion coatings on corrosion of aluminum alloy 2024-T3, *Surface Coatings and Technology, 140 (2001)* 1, pp. 51–57.

[3] Kulinich, S. A., Akhtar, A. S., On conversion coating treatments to replace chromating for Al alloys: Recent developments and possible future directions, *Russian Journal of Non-Ferrous Metals, 53 (2012)* 2 , pp. 176–203.

[4] Wang, D., Bierwagen, G. P., Sol-gel coatings on metals for corrosion protection, *Progress in Organic Coatings, 64 (2009)* 4, pp. 327–338.

[5] Lvov, Y., Wang, W., Zhang, L., Fakhrullin, R., Halloysite clay nanotubes for loading and sustained release of functional compounds, *Advanced Materials, 28 (2016)* 6, pp. 1227–1250.

[6] Wei, H., Wang, Y., Guo, J., Shen, N. Z., Jiang, D., Zhang, X., Yan, X., Zhu, J., Wang, Q., Shao, L., Lin, H., Wei, S., Guo, Z., Advanced micro/nanocapsules for self-healing smart anticorrosion coatings, *Journal of Materials Chemistry A, 3 (2015)* 2, pp. 469–480.

[7] Lanzara, G., Yoon, Y., Liu, H., Peng, S., Lee, WI., Carbon nanotube reservoirs for self-healing materials, *Nanotechnology, 20 (2009)* 33, pp. 335704

[8] Zheludkevich, M. L., Poznyak, S. K., Rodrigues, L. M,, Raps, Hack, T., Dick, L. F., Nunes, T . D., Ferreira, M. G. S., Active protection coatings with layered double hydroxide nanocontainers of corrosion inhibitor, *Corrosion Science 52 (2010)* 2, pp. 602–611.

[9] Manasa, S., Siva, T., Sathiyanarayanan, S., Gobi, K. V., Subasri, R., Montmorillonite nanoclay-based self-healing coatings on AA 2024-T4, *Journal of Coatings Technology and Research, 15 (2018)* 4, pp. 721–735.

[10] Darmiani, E., Rashed, G. R., Zaarei, D., Danaee, I., Synergistic effects of ntmorillonite/cerium nitrate additives on the corrosion performance of epoxy-clay nanocomposite coatings, *Polymer- Plastics Technology and Engineering, 52 (2013)* 10, pp. 980–990.

[11] Montemor, M. F., Snihirova, D. V., Taryba, M. G., Lamaka, S. V., Kartsonakis, I. A,, Balaskas, A. C., Kordas, G. C., Tedim, J., Kuznetsova, A., Zheludkevich, M. L., Ferreira, M. G.S., Evaluation of self-healing ability in protective coatings modified with combinations of layered double hydroxides and cerium molibdate nanocontainers filled with corrosion inhibitors, *Electrochimica Acta. 60 (2012),* pp. 31–40.

[12] Serdechnova, M., Kallip, S., Ferreira, M. G. S., Zheludkevich, M. L., Active self-healing coating for galvanically coupled multi-material assemblies, *Electrochemistry Communications. 41 (2014),* pp. 51–54.

[13] Manasa, S., Jyothirmayi, A., Siva, T., Sathiyanarayanan, S., Gobi, K. V., Subasri, R., Effect of inhibitor loading into nanocontainer additives of self-healing corrosion protection coatings on aluminum alloy A356.0, *Journal of Alloys and Compounds, 726 (2017),* pp. 969–977.

[14] Manasa, S., Jyothirmayi, A., Siva, T., Sarada, B. V., Ramakrishna, M., Sathiyanarayanan, S., Gobi, K.V., Subasri, R., Nanoclay-based self-healing, corrosion protection coatings on aluminum, A356.0 and AZ91 substrates, *Journal of Coatings Technology Research, 14 (2017)* 5, pp. 1195–1208.

[15] ASTM B117-16 Standard Practice for Operating Salt Spray (Fog) Apparatus, *(2016).*

[16] ASTM G31-12 Standard Guide for Laboratory Immersion Corrosion Testing of Metals 1, *(2012),* pp. 1–10.

[17] ASTM G1-90 Standard Practice for Preparing, Cleaning and Evaluation Corrosion Test Specimens, *(1999)* pp. 15-18.

[18] Huttunen-Saarivirta, E., Vaganov, G. V., Yudin, V. E., Vuorinen, J., Characterization and corrosion protection properties of epoxy powder coatings containing nanoclays, *Progress in Organic Coatings, 76 (2013)* 4, pp. 757–767.